

Strong Equivalence, Lorentz and CPT Violation, Anti-Hydrogen Spectroscopy and Gamma-Ray Burst Polarimetry

Graham M. Shore

Department of Physics

University of Wales, Swansea

Swansea SA2 8PP, U.K.

E-mail: g.m.shore@swansea.ac.uk

Abstract: The strong equivalence principle, local Lorentz invariance and CPT symmetry are fundamental ingredients of the quantum field theories used to describe elementary particle physics. Nevertheless, each may be violated by simple modifications to the dynamics while apparently preserving the essential fundamental structure of quantum field theory itself. In this paper, we analyse the construction of strong equivalence, Lorentz and CPT violating Lagrangians for QED and review and propose some experimental tests in the fields of astrophysical polarimetry and precision atomic spectroscopy. In particular, modifications of the Maxwell action predict a birefringent rotation of the direction of linearly polarised radiation from synchrotron emission which may be studied using radio galaxies or, potentially, gamma-ray bursts. In the Dirac sector, changes in atomic energy levels are predicted which may be probed in precision spectroscopy of hydrogen and anti-hydrogen atoms, notably in the Doppler-free, two-photon $1s \rightarrow 2s$ and $2s \rightarrow n$ ($n \geq 10$) transitions.

Contents

1. Introduction	1
2. Strong Equivalence Violating QED	4
2.1 Extended Maxwell action	5
2.2 Extended Dirac action	7
2.3 Energy-momentum tensor	8
3. Lorentz and CPT Violating QED	11
4. Astrophysical Polarimetry	14
4.1 Light propagation and birefringence	14
4.2 Radio galaxies	18
4.3 Gamma-ray bursts	19
5. Precision Atomic Spectroscopy	23
5.1 Hydrogen spectrum with Lorentz and CPT violation	23
5.2 $1s \rightarrow 2s$ and $2s \rightarrow nd$ ($n = 10$) transitions in H and anti-H	26
6. Conclusions	29

1. Introduction

The quantum field theories used to describe elementary particle physics incorporate a number of basic principles including Lorentz invariance, unitarity, causality, locality and CPT symmetry and, in the presence of gravity, the weak and strong equivalence principles. Although there are no compelling theoretical or experimental reasons to question these principles, it is nevertheless interesting to speculate on the experimental consequences should any of them turn out to be violated in nature.

In this paper, we consider modifications of the dynamics of QED exhibiting either violations of the strong equivalence principle or of Lorentz and CPT invariance and discuss certain experimental signatures, notably in the surprisingly related fields of precision hydrogen and anti-hydrogen spectroscopy and polarimetry of astrophysical sources such as radio galaxies or gamma-ray bursts.

The weak equivalence principle requires the existence at each spacetime point of a local inertial frame of reference. This is fundamental to the structure of general relativity and is realised by formulating spacetime as a (pseudo-)Riemannian manifold. We will keep this as the basis for quantum field theory in curved spacetime. The strong equivalence

principle, however, apparently has a rather different status, being simply a restriction on the dynamics of the theory. It requires that the laws of physics (i.e. dynamics) are identical in each of these local inertial frames, where they reduce to their special relativistic form. Precisely, this requires the matter fields to couple to gravity through the connections only (minimal substitution), not through direct couplings to the curvature tensors. Strong equivalence violation can therefore be realised by including in the QED Lagrangian interaction terms coupling the electromagnetic or Dirac fields directly to the curvature, e.g. $\frac{1}{2}M^2 R F_{\mu\nu} F^{\mu\nu}$ or $\frac{1}{2}M^2 R \bar{\psi} \gamma^\mu D_\mu \psi$. M is a characteristic mass scale for strong equivalence violation and is to be determined, or bounded, from experiment.

In the electromagnetic sector, it is known from the original work of Drummond and Hathrell[1] that terms of this type arise in the effective action for QED in curved spacetime as a result of integrating out electron loops. In this case, the mass scale M is simply the electron mass m and the coefficients are of order α , the fine structure constant. In previous work [1, 2, 3, 4, 5, 6], we have investigated at length the implications of this effective quantum-induced violation of the strong equivalence principle for photon propagation. By far the most interesting result is the apparent prediction of superluminal propagation of light. A careful review of this effect and its implications for causality has been given in refs.[6, 7], where it is shown that in general relativity, superluminal propagation may in fact be compatible with stable causality. The situation is complicated by the fact that the full effective action for QED in curved spacetime [6, 8] involves interactions and form factors depending on spacetime covariant derivatives in addition to the terms in the original Drummond-Hathrell action, e.g. $\frac{1}{4}M^4 R^2 D_\mu F_\nu D^\mu F^\nu$. This implies that light propagation is dispersive and the analysis of causality requires the identification of the relevant ‘speed of light’, which turns out to be identifiable as the high-frequency limit of the phase velocity [9].

In section 2, we construct a general strong equivalence violating QED Lagrangian in both the photon and electron sectors, keeping interactions of all orders in derivatives but, as above, only of first order in the gravitational curvature. The photon part of the Lagrangian is essentially the same as the effective action derived in ref.[8]. The electron Lagrangian, however, is quite new, although related to previous work on the propagation of massless neutrinos in a background gravitational field [10].

It is important to realise that, unlike the photon case, this electron Lagrangian does not have an interpretation as a low-energy effective action for QED – there is no way of ‘integrating out the photon field’ to leave a local, infra-red finite effective action describing electron propagation in curved spacetime. Nevertheless, we can relate our strong equivalence violating generalisation of the Dirac Lagrangian to previous analyses of the electron propagator in curved spacetime (more precisely, the evaluation of the electron matrix elements of the energy-momentum tensor) incorporating one-loop self-energy contributions [11, 12, 13].

Lorentz and CPT violating dynamics is introduced in a similar way. We begin as usual with the standard formulation of QED in Minkowski spacetime, but include tensor operators in the action multiplied by multi-index coupling constants, e.g. $K_{\mu\nu} F_{\mu\nu} F_{\mu\nu}$ or $c_{\mu\nu} \bar{\psi} \gamma^\mu D^\nu \psi$. Since these couplings are simply collections of constants, not tensor fields in their own right, Lorentz invariance is explicitly violated in the dynamics of this modified

QED. Although it is not necessary for this phenomenological approach, we can imagine these couplings to be Lorentz-violating VEVs of tensor fields in some more fundamental theory. This approach to Lorentz and CPT violation has been pioneered by Kostelecky [14], who has constructed the most general Lorentz-violating generalisation of the standard model incorporating renormalisable (dimension ≤ 4) operators. In an extended series of papers, Kostelecky and collaborators have examined in detail a great variety of potential experimental signatures of these new interactions. For a review, see, e.g. ref.[15].

The analogy between these Lorentz and CPT violating Lagrangians and the strong equivalence violating QED Lagrangian is clear, with, for example, the coupling constant K playing the role of the Riemann tensor R . It is therefore easy to translate aspects of the phenomenology of one theory to the other. As we shall see in section 4, this leads to some new insights and economy of analysis.

A novel feature of the Kostelecky Lagrangian is its inclusion, as a subset of the Lorentz-violating terms, of interactions that are CPT odd. We recall that CPT invariance is a general theorem of quantum field theory assuming the general principles of Lorentz invariance, locality and microcausality are respected (see, e.g. ref.[16]). The Kostelecky Lagrangian evades the CPT theorem by explicitly breaking Lorentz invariance. It therefore provides an interesting arena in which to study the possible experimental signatures of CPT violation. This is particularly important at present in view of the current experiments on antihydrogen spectroscopy which are designed to test the limits of CPT with unprecedented accuracy.

In the second part of this paper, we turn to some possible experimental consequences of these novel phenomenological Lagrangians. As we have already extensively investigated, the strong equivalence violating modifications to the QED Lagrangian have important consequences for photon propagation. The light cone is modified and in many cases superluminal propagation becomes possible. Moreover, if the Weyl tensor C (the trace-free part of the Riemann tensor) is non-vanishing, the effective light cone acquires a dependence on the polarisation, so that the speed of light becomes polarisation dependent. This is the phenomenon of gravitational birefringence. We immediately realise that the same birefringent effect will also arise with the Lorentz-violating Lagrangian [14], provided the coupling K has a trace-free component analogous to C . The Newman-Penrose formalism, which was found to be an elegant way of analysing results in the strong equivalence violating case, may similarly be usefully adapted to the Lorentz-violating Lagrangians.

One of the most important physical manifestations of birefringence is the rotation of the plane of linearly polarised light as it passes through the birefringent medium, in our case either the background gravitational field or, in the Lorentz-violating scenario, simply the vacuum. Since we expect any strong equivalence, Lorentz or CPT violations to be tiny, detection of this birefringent rotation requires experiments with the longest possible baseline, since the rotation angle will be proportional to the distance the light has propagated through the birefringent medium. This leads us to focus on astrophysical sources which emit radiation with a well-defined orientation of linear polarisation. A thorough analysis of this effect for the case of the CPT-violating Chern-Simons interaction $L_{CS} = \frac{1}{4} F_{\mu\nu} \tilde{F}^{\mu\nu}$ in the Kostelecky Lagrangian was performed some time ago by Carroll, Field and Jackiw [17],

who were able to bound the coupling L by placing limits on such a birefringent rotation from observations of synchrotron emission from radio galaxies. In section 4, we briefly review this and more recent work by Kostelecky and Mewes [18], then go on to discuss the possibility of improving these bounds by considering higher redshift sources, in particular by exploiting the linear polarisation observed in the afterglow of gamma-ray bursts to look for a Lorentz-violating birefringent rotation.

Curiously, while looking for strong equivalence, Lorentz and CPT violation in the photon sector requires experiments on astronomical scales, testing the electron sector is the domain of precision atomic spectroscopy. Even more intriguingly, since symmetry violation in the photon sector implies, through radiative corrections, a corresponding violation in the electron sector (and vice-versa), experimental bounds on the Kostelecky photon couplings K and L and the electron couplings a and b are in principle correlated. That is, bounds on Lorentz and CPT violation found from astrophysics may also constrain the violation of these symmetries in the experiments on anti-hydrogen spectroscopy. However, there are some caveats here related to subtle anomaly-related issues in QED [19], so the situation is actually not quite so clear-cut (see section 3).

In section 5, therefore, we address the question of strong equivalence, Lorentz and CPT violation in the electron sector of QED, using the appropriately modified Dirac equation to recalculate atomic energy levels and their implications for precision hydrogen and anti-hydrogen spectroscopy. Following the production of significant numbers of cold anti-hydrogen atoms by the ATHENA [20, 21] and ATRAP [22, 23] experiments at CERN, the potential of performing precision measurements of the anti-hydrogen as well as hydrogen spectrum may be realised, and it is hoped that experiments will soon be underway to test CPT to high accuracy by comparing the frequencies of the $1s \rightarrow 2s$ transition in hydrogen and anti-hydrogen. This transition is favoured because of the extremely narrow linewidth of the $2s$ state, since the only available decay is the Doppler-free, two-photon $1s \rightarrow 2s$ transition. However, within the framework of the Kostelecky Lagrangian, CPT violation would only be observable in the hyperfine Zeeman splittings of this transition for trapped anti-hydrogen [24], where the linewidths would be subject to Zeeman broadening. Here, we present a slightly extended analysis of the energy level shifts predicted by the modified Dirac equation and propose an alternative measurement which in practice may be of comparable accuracy, namely the Doppler-free, two-photon $2s \rightarrow n$ ($n \geq 10$) transition for hydrogen and anti-hydrogen.

2. Strong Equivalence Violating QED

The weak equivalence principle requires the existence of a local inertial frame at each spacetime point. This is realised by making spacetime a (pseudo-)Riemannian manifold, which admits a tangent space at each point, related to spacetime via the vierbein e_a^μ (where a is the tangent space index). In quantum field theory in curved spacetime, the fundamental fields are defined on this tangent space.

The strong equivalence principle is invoked to constrain the dynamics. It requires that the laws of physics are the same at the origin of the local inertial frame at each

spacetime point, where they reduce to their usual special relativistic form. This is realised by requiring the coupling of the fields to gravity to involve only the spacetime connection, not directly the curvature tensors. It is equivalent to minimal substitution, where the general relativistic equations of motion are found from the special relativistic ones by substituting the covariant derivatives for ordinary derivatives. The same principle is of course already used to construct the usual QED Lagrangian itself (the electron field is coupled to electromagnetism via the gauge covariant derivative only, with the (non-renormalisable) operators coupling bilinears directly to the field strength F being omitted). The conventional QED action is therefore simply

$$\int d^4x \sqrt{-g} \left[-\frac{1}{4} F_{ab} F^{ab} + i e \bar{\psi} \gamma^a D_a \psi - m \bar{\psi} \psi \right] \quad (2.1)$$

where $D_a = (\partial_a + \frac{i}{2} \omega_{ab} \sigma^{ab} + i e A_a)$ is the covariant derivative, involving the spin connection $\omega_{ab} = e_a^\mu (\partial_\mu e_b - \partial_b e_\mu)$. Here, $\sigma^{ab} = \frac{i}{4} [\gamma^a, \gamma^b]$, and in what follows we shall usually abbreviate $\gamma^a = e_a^\mu \gamma_\mu$.

2.1 Extended Maxwell action

The strong equivalence principle is violated by the introduction of direct couplings to the curvature tensors R_{ab} ; R and R^2 , e.g. $\frac{1}{M^2} R F_{ab} F^{ab}$. This implies that the local dynamics now distinguishes between spacetime points, since it obviously depends on the curvature at each point. Since these new interactions necessarily involve non-renormalisable ($\dim > 4$) operators, their inclusion introduces a new scale M , which in our phenomenological approach characterises the scale of strong equivalence violation. Its value is to be determined, or bounded, by experiment.

We will only consider operators which are linear in the curvature. This is most naturally interpreted as keeping only the lowest-order terms in an expansion of a more general Lagrangian in $O(R/M^2)$, so we regard the resulting theory as a valid approximation for gravitational fields which are weak on the scale M . On the other hand, we will write down an action which involves all orders in covariant derivatives acting on the fields. In this case, keeping only terms of lowest order in $O(D^2/M^2)$ is a low-momentum (or low-frequency) approximation. This will nevertheless be a useful first step in understanding the phenomenology of strong equivalence violation.

A systematic analysis of all possible $O(R/M^2)$ operators shows that the most general strong equivalence violating extension of the Maxwell sector of QED at this order has the action

$$\begin{aligned} = \int d^4x \sqrt{-g} & \left[-\frac{1}{4} F_{ab} F^{ab} + \frac{1}{M^2} D_a F^a \quad \frac{1}{M^2} D_a D^a F \right. \\ & + \frac{1}{M^2} a_0 R F_{ab} F^{ab} + \frac{1}{M^2} b_0 R F^a{}_b F^b{}_a + \frac{1}{M^2} c_0 R F_{ab} F^{ab} \\ & + \frac{1}{M^4} \frac{1}{M^4} a_1 R D_a F^a{}_b D^b{}_c F^{cd} + \frac{1}{M^4} b_1 R D_a F^a{}_b D^b{}_c D^c{}_d F^{de} \\ & \left. + \frac{1}{M^4} b_2 R D_a D_b F^a{}_c D^c{}_d F^{de} + \frac{1}{M^4} b_3 R D_a D_b D_c F^a{}_d F^{de} \right] \end{aligned}$$

$$+ \frac{1}{M^6} \dot{c}_1 R_{\alpha\beta\gamma\delta} F^{\alpha\beta} F^{\gamma\delta} + \frac{1}{M^6} \dot{b}_4 R_{\alpha\beta\gamma\delta} F^{\alpha\beta} F^{\gamma\delta} \quad (2.2)$$

In this formula, the $\dot{a}_n, \dot{b}_n, \dot{c}_n$ are form factor functions of three operators, i.e.

$$\dot{a}_n = a_n \left(\frac{D_{(1)}^2}{M^2}; \frac{D_{(2)}^2}{M^2}; \frac{D_{(3)}^2}{M^2} \right) \quad (2.3)$$

where the first entry ($D_{(1)}^2$) acts on the first following term (the curvature), etc. \dot{a}_0 is similarly defined as a single variable function.

To establish eq.(2.2), extensive use has been made of the Bianchi identities for the electromagnetic field strength and the curvature tensors, viz. $D_{[\alpha} F_{\beta\gamma]} = 0$; $D_{[\alpha} R_{\beta\gamma]\delta\epsilon} = 0$; $D_{\alpha}(R_{\beta\gamma} - \frac{1}{2}Rg_{\beta\gamma}) = 0$, the commutation relation $[D_{\alpha}; D_{\beta}] = O(R)$ for covariant derivatives, and repeated use of integration by parts to show the equivalence in the action of different operators. As a simple illustration, notice for example that

$$\int d^4x R_{\alpha\beta\gamma\delta} F^{\alpha\beta} F^{\gamma\delta} = \int d^4x R_{\alpha\beta\gamma\delta} F^{\alpha\beta} F^{\gamma\delta} + \frac{1}{4} \int d^4x D^2 R F_{\alpha\beta} F^{\alpha\beta} \quad (2.4)$$

so the apparently independent operator on the l.h.s. is equivalent to a combination of the b_2 and b_0 terms, taking account of the form factors.¹

In applications of eq.(2.2), in particular to the analysis of birefringence in section 4, it is often convenient to introduce the Weyl tensor $C_{\alpha\beta\gamma\delta}$. Indeed, it is only the Weyl tensor contribution which gives rise to birefringence. Explicitly, $C_{\alpha\beta\gamma\delta}$ is the trace-free part of the Riemann tensor:

$$C_{\alpha\beta\gamma\delta} = R_{\alpha\beta\gamma\delta} - \frac{1}{2}(R_{\alpha\gamma}g_{\beta\delta} + R_{\beta\delta}g_{\alpha\gamma} - R_{\alpha\delta}g_{\beta\gamma} - R_{\beta\gamma}g_{\alpha\delta}) + \frac{1}{6}R(g_{\alpha\gamma}g_{\beta\delta} - g_{\alpha\delta}g_{\beta\gamma}) \quad (2.5)$$

In contrast to the Ricci tensor $R_{\alpha\beta}$, the Weyl tensor is not directly constrained by matter via the Einstein field equations. The two operators involving the Riemann tensor in eq.(2.2) can be re-expressed in terms of the Weyl tensor and combinations of the Ricci tensor and Ricci scalar terms as follows. (Note that these identities hold only under the integral and to $O(R)$.)

$$\int d^4x \sqrt{-g} C_{\alpha\beta\gamma\delta} F^{\alpha\beta} F^{\gamma\delta} = \int d^4x \sqrt{-g} R_{\alpha\beta\gamma\delta} F^{\alpha\beta} F^{\gamma\delta} - 2R_{\alpha\beta} F^{\alpha\gamma} F^{\beta\gamma} + \frac{1}{3}R F_{\alpha\beta} F^{\alpha\beta} \quad (2.6)$$

and

¹Notice that in the effective action in ref.[6, 8], $\int d^4x R_{\alpha\beta\gamma\delta} F^{\alpha\beta} F^{\gamma\delta}$ and $\int d^4x R_{\alpha\beta} F^{\alpha\gamma} F^{\beta\gamma}$ were included as independent terms. The effective action quoted there can therefore be simplified. They do, however, arise from the quite different operators $\text{tr} R_{\alpha\beta} F^{\alpha\gamma} F^{\beta\gamma}$ and $\text{tr} R_{\alpha\beta} \hat{F}^{\alpha\gamma} \hat{F}^{\beta\gamma}$ in the Barvinsky et al. action for general background fields [25, 26].

$$\int d^4x \sqrt{-g} \left(\frac{1}{2} F_{\mu\nu} F^{\mu\nu} + \frac{1}{4} R F_{\mu\nu} F^{\mu\nu} + \frac{1}{6} R^2 F_{\mu\nu} F^{\mu\nu} + \frac{1}{4} R D_\mu F^\mu{}_\nu D^\nu{}_\rho F^\rho{}_\sigma + \frac{1}{4} R D_\mu D_\nu F^\mu{}_\rho F^\rho{}_\sigma \right) \quad (2.7)$$

While in this paper we are considering eq.(2.2) as a phenomenological Lagrangian exhibiting violation of the strong equivalence principle, it is important to realise that the same expression (with M interpreted as the electron mass) arises in conventional QED in curved spacetime as the effective action for the electromagnetic field when we include one-loop vacuum polarisation to integrate out the electron field. It is therefore the appropriate action to use to study photon propagation in curved spacetime, taking into account quantum effects at $O(\hbar)$. There is just one difference: at one-loop, the quantum effective action does not have the $O(1/M^6)$ term that we have included above. Exact expressions for the form factors derived in QED at $O(\hbar)$ are known and are given in ref.[8].

2.2 Extended Dirac action

A similar analysis can be carried out to find the most general free Dirac action comprising strong equivalence breaking operators of first order in the curvature but all orders in derivatives. A systematic study of all the possibilities shows that the following is a complete basis:

$$\begin{aligned} &= \int d^4x \sqrt{-g} \left(i \bar{\psi} \not{D} \psi - m \bar{\psi} \psi \right) + \frac{1}{M} \int d^4x \sqrt{-g} \left(h_1 D^2 \bar{\psi} \psi + i h_2 D^2 \bar{\psi} \not{D} \psi \right) \\ &+ \frac{1}{M} \int d^4x \sqrt{-g} \left(f_1 R \bar{\psi} \psi + \frac{1}{M^2} \left(f_2 i R \bar{\psi} \not{D} \psi + f_3 i R D_\mu \bar{\psi} \psi \right) + \frac{1}{M^3} f_4 i R D_\mu \bar{\psi} \not{D} \psi \right) \\ &+ \frac{1}{M^2} \int d^4x \sqrt{-g} \left(g_1 i R \bar{\psi} \not{D} \psi + \frac{1}{M^3} \left(g_2 R \bar{\psi} \not{D} \psi + g_3 i R D_\mu \bar{\psi} \not{D} \psi \right) \right) \\ &+ \frac{1}{M^4} \int d^4x \sqrt{-g} \left(g_4 i R D_\mu \bar{\psi} \not{D} \psi + g_5 i R D_\mu \bar{\psi} \not{D} \psi \right) \\ &+ \frac{1}{M^5} \int d^4x \sqrt{-g} \left(g_6 i R D_\mu \bar{\psi} \not{D} \psi + \dots \right) + h.c. \end{aligned} \quad (2.8)$$

where as before the f_n , g_n and h_n are form factor functions of derivatives.

A notable feature of eq.(2.8) is that there is no independent term involving the Riemann tensor. That is, there is no possible term in the action that can be built from the trace-free Weyl tensor. This follows relatively straightforwardly from the symmetries of $R_{\mu\nu}$ and the (Bianchi) identity $D_\mu R_{\nu\rho} = D_\nu R_{\mu\rho} - D_\rho R_{\mu\nu}$. The independence of this Dirac action on the Weyl tensor is in marked contrast to the Maxwell action.

At first sight, it might be thought that just as the extended Maxwell action can be realised as the quantum effective action governing photon propagation in the presence of vacuum polarisation, this extended Dirac action could similarly be realised as an effective action for electrons incorporating one-loop self-energy corrections in the presence of gravity. In fact, there is no local effective action which accomplishes this[13]. The reason is that

whereas it makes sense to write a low-energy effective Lagrangian valid below the scale of the electron mass, it is not possible to do the same with the massless photon. If we try, we find that the form factors f_i, g_i, h_i in the Dirac action cannot be local, i.e. polynomial functions in D^2 . As we see below, their Fourier transforms include infra-red singular logarithms of momentum.

On the other hand, a slight generalisation of eq.(2.8) to chiral fermions is a good effective action for the propagation of neutrinos in curved spacetime. In this case, the relevant one-loop self-energy diagrams involve the W or Z boson propagators and the quantum corrections can be encoded at low energies by an effective action for the neutrinos alone, with the strong equivalence breaking scale M being identified with the weak scale m_W . An analysis of neutrino propagation in curved spacetime has been carried out some time ago by Okukuwa [10], generalising the results of Drummond and Hathrell [1] for photons. To lowest order in curvature and for low-momentum neutrinos, he finds that the $\bar{h}_1; \bar{f}_2; \bar{f}_3$ and \bar{g}_1 operators, modified to include left-handed chiral propagators and with constant coefficients of $O(=m_W)$, are sufficient to encode the one-loop self-energy corrections, and computes the $g_1(0;0;0)$ coefficient (the only one which affects the neutrino velocity). Just as in the photon case, this allows the possibility of superluminal propagation of (massless) neutrinos in certain spacetimes, notably the FRW universe. However, whereas there is a birefringent shift in the photon velocity (with one polarisation being superluminal) for Ricci-flat spacetimes such as the Schwarzschild black hole, the neutrino velocity remains equal to the speed of light in this case. Our construction of the general Dirac action (2.8) shows that in fact this is a general result, valid beyond the low-momentum approximation.

Eq.(2.8) can easily be extended to include electron-photon interactions by promoting the spacetime covariant derivatives to be gauge covariant as well. As explained above, this is the conventional prescription of minimal substitution which, in ordinary QED, ensures a renormalisable Lagrangian. It could reasonably be argued, however, that in the spirit of constructing (non-renormalisable) strong equivalence violating phenomenological extensions of QED, we should also allow violation of the gauge minimal substitution principle as well and include operators coupling the electron bilinears directly to the electromagnetic field strength F as well as the spacetime curvatures. Examples of such interactions would be $\bar{\psi} \gamma^\mu D_\mu \psi$ or $\bar{\psi} \gamma^\mu \psi F_{\mu\nu} F^{\mu\nu}$. Since we will not make use of such interactions in this paper, however, we will not present a classification of all such possibilities here.

2.3 Energy-momentum tensor

After reviewing the analogous formalism for broken Lorentz and CPT violation in the next section, we shall discuss the implications of these extended Maxwell and Dirac actions for the propagation of polarised light and for atomic spectroscopy in sections 4 and 5 respectively.

First, though, we shall evaluate the electron matrix element of the energy-momentum tensor using the Dirac action (2.8). This is an important object in several contexts, ranging from the study of general relativity as a low-energy effective theory of quantum gravity [13] to deep inelastic scattering, where the energy-momentum tensor arises in the operator product expansion of electromagnetic currents and the form factors are identified as structure

functions (the matrix elements being taken between proton rather than electron states). It is also important in determining the explicit expressions for the form factors in any application where the extended Dirac action can be viewed as a conventional low-energy effective action, e.g. in the generalisation to neutrino propagation. So while the discussion that follows is rather formal, the results may have applications in a number of interesting contexts.

The energy-momentum tensor matrix element in flat spacetime is defined as

$$\langle p^0 | T_{\mu\nu} | p^0 \rangle = \frac{1}{2} \frac{1}{g} \frac{\delta^3}{\delta g^{\mu\nu}} \ln Z = \frac{1}{2} \frac{\delta}{\delta g^{\mu\nu}} \ln Z \quad (2.9)$$

which follows immediately from the definition of $T_{\mu\nu}$ as the functional derivative of the action with respect to the metric. Interpreted in perturbative quantum gravity, this is the electron-graviton vertex.

Its evaluation therefore amounts to taking the metric variation of the various terms in the extended Dirac action. We therefore collect here some useful formulae for functional derivatives:

$$\frac{\delta}{\delta g^{\mu\nu}} (g^{\mu\nu}) = \frac{1}{2} g^{\mu\nu} \quad (2.10)$$

$$\frac{\delta}{\delta g^{\mu\nu}} R(g) = R(g) + g^{\mu\nu} \frac{\delta R}{\delta g^{\mu\nu}} \quad (2.11)$$

$$\frac{\delta}{\delta g^{\mu\nu}} R(g) = \frac{1}{2} g^{\mu\nu} \frac{\delta R}{\delta g^{\mu\nu}} + g^{\mu\nu} \frac{\delta R}{\delta g^{\mu\nu}} \quad (2.12)$$

where, importantly, the derivatives are w.r.t. x .

Acting on spinor quantities, the metric derivative is to be re-interpreted in terms of the vierbein as

$$\frac{\delta}{\delta g^{\mu\nu}} = \frac{1}{4} e_c^\mu \frac{\delta}{\delta e_c^\nu} + e_c^\nu \frac{\delta}{\delta e_c^\mu} \quad (2.13)$$

Recalling that the vanishing of the covariant derivative of the vierbein

$$D_\mu e_b^\nu = \partial_\mu e_b^\nu + \omega_{\mu b}^c e_c^\nu = 0 \quad (2.14)$$

defines the spin connection as

$$\omega_{\mu ab} = e_a^\nu \partial_\mu e_{b\nu} - e_b^\nu \partial_\mu e_{a\nu} \quad (2.15)$$

where \tilde{D} is covariant only w.r.t. the curved spacetime index, we can also show that

$$\frac{1}{4} e_c^\mu(x) \frac{\delta}{\delta e_c^\nu(x)} + e_c^\nu(x) \frac{\delta}{\delta e_c^\mu(x)} = \frac{1}{2} \tilde{D}^\mu e^\nu_a e^\mu_b \quad (2.16)$$

where, again, the derivative is w.r.t. x . Note that in this formalism, the connection is considered as independent of the vierbein e_a . With this interpretation, we can then

readily check that the energy-momentum tensor for the conventional Dirac action is simply

$$\begin{aligned} T &= \frac{2}{g} \frac{1}{g} \int d^4x \sqrt{-g} (i \bar{\psi} \not{D} \psi) + \text{h.c.} \\ &= \frac{1}{2} \int d^4x \sqrt{-g} (i \bar{\psi} \not{D} \psi) \end{aligned} \quad (2.17)$$

The matrix elements of each of the terms in eq.(2.8) can now be taken in turn. For those already involving a curvature tensor, the only contributions to the flat spacetime matrix elements are clearly those arising from the variations of the curvature tensors themselves using eqs.(2.11),(2.12). For these terms, therefore, we do not need to take the metric variations of the form factors themselves. We do, however, need to take into account the variations of the h_i form factors.

The matrix element $\bar{u}(p) \Gamma(q) u(p)$, or electron-graviton vertex, can be easily shown to have only three possible independent Lorentz structures in momentum space. Each of these individually satisfies the conservation constraint $q \cdot T = 0$, which follows from diffeomorphism invariance of the action, using the equations of motion for the on-shell wave functions $u(p), u(p^0)$. (The kinematical variables used here are $p = (p^0)$ for the initial (nal) electron momenta and $q = p^0 - p$ for the momentum transfer (graviton momentum)). We can choose them to be $(\not{P} + \not{P})$; $\not{P} \not{P}$ and $(q \cdot q - q^2 g)$, where $P = \frac{1}{2}(p^0 + p)$. The form factors f_i, g_i reduce on-shell to single functions of the momentum transfer squared, i.e.

$$f_i \equiv f_i(q^2; p^0; p^2)_{\text{on shell}} = f_i(q^2) \quad (2.18)$$

To simplify notation, we also let $h_i(q^2) = q^2 h_i^0(q^2) = \tilde{h}_i(q^2)$.

Notice that the set of Lorentz structures chosen here is not unique. Another frequently used basis replaces the term $(\not{P} + \not{P})$ by $\frac{1}{m}(\not{q} \not{P} + \not{P} \not{q})$. The translation between the two can be made using the Gordon identity

$$\frac{1}{m} \bar{u}(p^0) \not{q} u(p) = \bar{u}(p^0) \not{P} u(p) \quad (2.19)$$

In order to simplify the analysis, we now choose to identify the strong equivalence breaking scale M with the electron mass m so that there is only one mass scale in the problem. This could easily be relaxed of course for a specific application. For example, for neutrino propagation we would take $M = m_W$ and neglect the neutrino mass compared to the weak scale. Putting all this together, we then find after an extensive calculation:

$$\begin{aligned} \bar{u}(p^0) \Gamma(q) u(p) &= \bar{u}(p^0) \left[\frac{1}{2} (\not{P} + \not{P}) + \tilde{h}_2 \frac{1}{2m^2} \not{q} \not{q} + \frac{1}{4m^2} \not{q} \not{q} \right. \\ &\quad + \frac{1}{m} \not{P} \not{P} - 2(\tilde{h}_1 + \tilde{h}_2) \frac{q^2}{m^2} (\not{g}_2 + \not{g}_4 + \frac{1}{2} \not{g}_3) - \frac{1}{4m^4} \not{g}_6 \\ &\quad \left. + \frac{1}{m} (q \cdot q - q^2 g) (\tilde{h}_1 + \tilde{h}_2) + 4(\tilde{f}_1 + \tilde{f}_2 - \frac{1}{4m^2} \tilde{f}_4) \right] u(p) \end{aligned}$$

$$\frac{1}{2} \frac{q^2}{m^2} (g_2 + g_4 + \frac{1}{2} g_3) + \frac{1}{8} \frac{q^4}{m^4} g_6 + \dots u(p) \quad (2.20)$$

This expression shows clearly how the various possible terms in the general extended Dirac action contribute to the three independent form factors in the energy-momentum tensor matrix element.

Expressions of this type have appeared several times in the literature as the $O(\hbar)$ contributions of one-loop electron self-energy diagrams in QED in the presence of a weak perturbation $g = \eta + \hbar$ of the Minkowski spacetime metric, i.e. as the QED corrections to the electron-graviton vertex in perturbative quantum gravity. Explicit expressions for the functions $F_1(q^2)$, $F_2(q^2)$ and $F_3(q^2)$ defined as the functions in square brackets in eq.(2.20) have been given for QED by several authors[11, 12, 13]. For small momentum transfer, the results are

$$F_1 = 1 - \frac{q^2}{4m^2} - \frac{47}{18} + \frac{2}{2} \frac{p \cdot m}{q^2} + \frac{2}{3} \ln \frac{q^2}{m^2} + \dots \quad (2.21)$$

$$F_2 = \frac{q^2}{4m^2} - \frac{4}{9} - \frac{2}{4} \frac{p \cdot m}{q^2} - \frac{4}{3} \ln \frac{q^2}{m^2} + \dots \quad (2.22)$$

$$F_3 = \frac{11}{4} - \frac{11}{9} - \frac{2}{2} \frac{p \cdot m}{q^2} - \frac{4}{3} \ln \frac{q^2}{m^2} + \dots \quad (2.23)$$

The $O(1)$ term in F_1 , which follows directly from the free Dirac action, can readily be seen to be a consequence of momentum conservation.

These expressions illustrate the essential problem in regarding the extended Dirac action too literally as a low-energy effective action in the usual sense. The non-analytic terms $\frac{p \cdot m}{q^2}$ and $\ln(q^2)$ are the signature of the long-range interactions in QED mediated by the massless photon. These interactions clearly cannot be 'integrated out'. However, they do carry important physical information and, as shown recently in ref.[13], can be used to reconstruct both classical and quantum corrections to the Kerr-Newman and Reissner-Nordstrom metrics.

The presence of non-analytic terms in the form factors for the energy-momentum tensor matrix elements prevents us from using eqs.(2.21), (2.22) and (2.23) to reconstruct polynomial form factors f_i , g_i and h_i in the extended Dirac action and view it as a true local effective action for QED in the same way as we have done for the extended Maxwell action. This programme could be carried out, however, with the chiral extension of the action where the scale M is taken as the vector boson mass m_W and the result interpreted as the effective action for neutrino propagation. In this case, the self-energy quantum corrections can indeed be encoded in an effective action of this type and a generalisation of eq.(2.20) could be used, as in the work of Ohkuwa[10], to constrain the f_i , g_i and h_i form factors by comparing with the results of explicit Feynman diagram calculations of the electron-graviton vertex in a Minkowski spacetime background.

3. Lorentz and CPT Violating QED

Lorentz invariance and CPT symmetry are fundamental properties of conventional quan-

tum field theories. Nevertheless, it is interesting to speculate that they may not be exact in nature and to study possible signatures for their violation, if only to stimulate increasingly precise experimental tests. A formalism for studying Lorentz and CPT violation within the framework of the standard model has been proposed and extensively explored in recent years by Kostelecky and collaborators [14, 15]. In this section, we briefly review this approach, emphasising the close technical similarities to our own work on strong equivalence violation.

In the Kostelecky approach, explicit Lorentz violation is introduced by writing a phenomenological Lagrangian comprising tensor operators with coupling constants carrying spacetime indices. These couplings are simply collections of numbers, not tensor fields in their own right. However, they may, though this is not at all necessary in the phenomenological approach, be thought of as Lorentz-violating VEVs of tensor fields in some more fundamental theory exhibiting spontaneous Lorentz violation. Restricting to renormalisable interactions, the most general such extension of QED is therefore (changing the notation of ref. [14] slightly):

$$\begin{aligned}
= & \int d^4x \left[\frac{1}{4} F_{\mu\nu} F^{\mu\nu} + (i \bar{\psi} \not{D} \psi) \right. \\
& + K \frac{1}{4} F_{\mu\nu} F^{\mu\nu} + \frac{1}{4} L_{\mu\nu} F^{\mu\nu} \\
& \left. + a \bar{\psi} \psi + b \bar{\psi} \gamma_5 \psi + i c \bar{\psi} \not{D} \psi + i d \bar{\psi} \gamma_5 \not{D} \psi + \frac{1}{2} h \bar{\psi} \psi \right] \quad (3.1)
\end{aligned}$$

With this notation, the couplings a, b, L of the super-renormalisable operators have dimensions of mass while c, d, h, K are dimensionless.

Here, we follow Kostelecky and restrict attention to the simple renormalisable Lagrangian (3.1). Of course, nothing prevents us from introducing further higher dimensional operators, particularly those with extra derivatives analogous to eqs. (2.2) and (2.8). This would be in the spirit of regarding this phenomenological action as a low-energy effective action in a theory in which Lorentz symmetry is broken at a high scale M .

Since Lorentz invariance is explicitly broken in (3.1), one of the axioms of the CPT theorem is not respected and therefore CPT symmetry is no longer guaranteed. In fact, the super-renormalisable operators with couplings a, b, L are CPT odd, while c, d, h, K multiply CPT even renormalisable operators. A phenomenological model of CPT violation is therefore obtained by using the Lagrangian (3.1) with the couplings a, b or L non-zero. It should also be noticed that in comparing results derived with positrons and electrons, the substitutions $a \rightarrow -a, d \rightarrow -d$ and $h \rightarrow -h$ should be made with the other couplings unchanged.

Now, it is evident that the Lorentz-violating QED Lagrangian (3.1) and the strong equivalence violating extended QED Lagrangians (2.2), (2.8) have many formal similarities. Tensor operators appear in each, though the role of the curvature tensors in eqs. (2.2), (2.8) is played by the multi-index, but non-tensorial, coupling constants in eq. (3.1). Notice also that the Lagrangian (3.1) allows for parity-violating operators which we chose to exclude from (2.2), (2.8). These would not occur in the quantum effective action obtained

from QED itself since this theory is parity-preserving, but could be included in a purely phenomenological theory. It follows that the analysis of the phenomenological consequences of the two theories will be very similar, and many results and predictions can simply be transcribed between them. We may also hope that some extra insight may be gained from this comparison. The couplings which admit a direct equivalence are:

$$\begin{array}{ll} a & f_3 D_R = M^2 \\ c & g_1 R = M^2 \\ K & c_0 R = M^2 \end{array} \quad (3.2)$$

Of the others, b , d and L are associated with the parity-violating operators which are not included in eqs.(2.2), (2.8). There is also no immediate analogue of the h term since R is symmetric and cannot couple to the operator without higher derivatives.

Probably the most useful correspondence is of the set of couplings K with the Riemann tensor R . K inherits the algebraic symmetries of the operator F^2 , which exactly matches the Riemann tensor. Just as we found it convenient to separate the Riemann tensor into the Ricci tensor and the trace-free Weyl tensor, so it will be useful to split K in the same way, defining the traced components K and K and the trace-free components $C^{(K)}$ using the same formula (2.5) that defines the Weyl tensor. We will see in the next section, where we go further and introduce the Newman-Penrose formalism, that this is a useful analogy to exploit in the analysis of the birefringent propagation of light.

In the remainder of the paper, we investigate some of the experimental consequences of this Lorentz and CPT violating Lagrangian, emphasising wherever possible the similarities, and differences, with the strong equivalence violating curved spacetime Lagrangian. First, though, we make some remarks about radiative corrections. It will be clear that if we take the modified electron propagator from the Dirac sector of (3.1) and substitute it into the one-loop photon vacuum polarisation diagram, it will produce a change in the photon propagator which can be realised as an $O(\epsilon)$ contribution to the coefficients of the Maxwell sector operators. And vice-versa, modifications of the photon propagator induce $O(\epsilon)$ contributions to the couplings of the Dirac sector operators. The result is that the electron and photon sector couplings are correlated by $O(\epsilon)$ radiative corrections. Exactly the same is of course true for the strong equivalence violating action.

It follows that if we are able to put a bound on the Dirac couplings a , b , c , d , h from experiments on atomic spectroscopy, then this will imply bounds on the Maxwell couplings K , L which are tested in astrophysical polarimetry experiments. And conversely, known bounds from astrophysics could imply bounds on future precision hydrogen and antihydrogen spectroscopy experiments, such as those planned by ATHENA and ATRAP at CERN. The possibility that astrophysics and atomic spectroscopy experiments could be correlated in this way was one of the principal motivations for this paper.

Perhaps the most interesting of these correlations would be those involving operators which give rise to CPT violation in the antihydrogen spectrum. In particular, consider

the parity-violating Dirac coupling b . At first sight, this appears to be linked via radiative corrections with the coupling L of the Chern-Simons operator. Since, as we see in the next section, the Chern-Simons term predicts a birefringent rotation of linearly polarised light which could in principle be observed in the synchrotron radiation from radio galaxies, we are able to place bounds on L from astrophysics. We would therefore expect this to imply a bound on b , which would limit the size of CPT violation which would be observed in the spectroscopic measurements at ATHENA and ATRAP.

Curiously though, the radiative correspondence between the axial-vector operator coupling b and the Chern-Simons coupling L is far from straightforward theoretically. The question of whether a Chern-Simons term is induced via the one-loop vacuum polarisation diagram where the fermion propagator is modified to include an axial-vector coupling turns out to be a subtle one in quantum field theory, involving ambiguities associated with the axial anomaly. A very careful analysis of this issue has been carried out by Jackiw and Kostecky [19], who conclude that the question "is a Chern-Simons term induced by vacuum polarisation in the theory with the Dirac action modified by an axial-vector term" has in fact no unique answer. Depending on how we attempt to give a definition of the theory taking proper account of the axial anomaly, a variety of reasonable answers may be given, including that the induced $L = \frac{3}{4}b$, 0 , or simply indeterminate.

In view of this interesting but indeterminate theoretical situation, it would therefore be unwise to place too much confidence on a prediction of a bound for CPT violation in antihydrogen based on the bound from radio galaxies.

4. Astrophysical Polarimetry

We now turn to the phenomenological consequences of the strong equivalence, Lorentz and CPT violating Lagrangians introduced so far. In this section, we focus on the photon sector and in particular on the polarisation dependence of the propagation of light (including radio waves and gamma-rays) in astrophysics.

4.1 Light propagation and birefringence

We begin with a brief review of light propagation based on the strong equivalence violating Lagrangian (2.2). This has been studied extensively in a series of papers [1, 2, 3, 4, 5, 6, 7] where we have explored the possibility of superluminal propagation and its implications for causality as well as gravitational birefringence and dispersion. The dispersive nature of light propagation, which as explained in ref.[6, 7] is essential in a precise analysis of causality and possible superluminal signal propagation, only becomes apparent when the full effective action (2.2) including the higher derivative operators is used. On the other hand, the basic features of gravitational birefringence are already apparent in the low-momentum approximation to the action first derived by Drummond and Hathrell[1]. In this section, we will restrict ourselves to this simple case. This is also most directly analogous to the Kostecky Lagrangian (3.1) with its restriction to renormalisable operators only.

To study the propagation of light in this theory, we use the formalism of geometric optics. The electromagnetic field is written in the form $A = A_0 \exp i$, where A_0 is the

amplitude and a is the polarisation vector. The amplitude is taken to be slowly-varying on the scale of the rapidly-varying phase θ . The wave-vector (equivalent up to some subtleties[7] to the photon momentum) is identified as $k = \partial \theta$. The essential features of light propagation are then obtained from the equations of motion of the extended Maxwell action by considering the highest order terms in a controlled expansion in the rapidly-varying quantities. All this formalism is explained in our previous papers (see [27] for a pedagogical review). The result is the following equation for the wave vector k and polarisation a :

$$k^2 a - k^\alpha a_k - \frac{2b + 4c}{M^2} R_{\alpha\beta} k^\alpha k^\beta a - k^\alpha k^\beta a - \frac{8c}{M^2} C_{\alpha\beta\gamma\delta} k^\alpha k^\beta a^\gamma = 0 \quad (4.1)$$

where a, b, c are coupling constants given from eq.(2.2) as $a = a_0(0;0;0)$, etc., and we have explicitly introduced the Weyl tensor. The modified light cone follows immediately from the condition

$$\det k^2 g_{\alpha\beta} - k^\alpha k^\beta - \frac{2b + 4c}{M^2} R_{\alpha\beta} - k^\alpha k^\beta - \frac{8c}{M^2} C_{\alpha\beta\gamma\delta} k^\gamma k^\delta = 0 \quad (4.2)$$

The physical light cone for photon propagation therefore no longer coincides with the geometric light cones of the background curved spacetime, and so eq.(4.2) predicts that the speed of light will be different from the fundamental 'speed of light' constant $c = 1$. The remarkable feature implied by (4.2) is that in some cases it predicts that the speed of light may be greater than 1, i.e. light propagation may be superluminal. For a careful discussion of what this means physically, we refer to our earlier papers[6, 7]. The second main prediction of eqs.(4.1), (4.2) is gravitational birefringence, viz. that the physical light cone (speed of light) will depend on the polarisation if, and only if, the Weyl tensor is non-vanishing. See below for an explicit demonstration.

As we have seen in earlier work, it is particularly useful in studying the implications of eqs.(4.1), (4.2) to adopt the Newman-Penrose formalism. (See ref.[4] for a relevant summary.) This involves introducing a null tetrad at each spacetime point via a set of null vectors l, n, m, \bar{m} satisfying $l^\alpha l_\alpha = 1; m^\alpha m_\alpha = -1; l^\alpha m_\alpha = \bar{m}^\alpha n_\alpha = n^\alpha m_\alpha = 0$. All tensors are then specified by their components in this basis. In the discussion below, we will take l as the direction of propagation, so that $k = \omega l$. $m = \frac{1}{\sqrt{2}}(a + ib)$ is a complex linear combination of two spacelike vectors transverse to l . It follows that m and \bar{m} represent respectively left and right-handed circular polarisation vectors, i.e. the photon helicity ± 1 eigenstates. The ten independent components of the Weyl tensor are described in the Newman-Penrose formalism by five complex scalars ψ_i ($i = 0, \dots, 4$), where

$$\begin{aligned} \psi_0 &= C_{\alpha\beta\gamma\delta} l^\alpha m^\beta l^\gamma m^\delta \\ \psi_1 &= C_{\alpha\beta\gamma\delta} l^\alpha n^\beta l^\gamma m^\delta \\ \psi_2 &= C_{\alpha\beta\gamma\delta} l^\alpha m^\beta m^\gamma n^\delta \\ \psi_3 &= C_{\alpha\beta\gamma\delta} l^\alpha n^\beta m^\gamma n^\delta \\ \psi_4 &= C_{\alpha\beta\gamma\delta} n^\alpha m^\beta n^\gamma m^\delta \end{aligned} \quad (4.3)$$

with similar definitions for the ten independent components of the Ricci tensor. Here, we only need the notation $\epsilon_{00} = \frac{1}{2}R_{\mu\mu}$.

Applying this formalism to eq.(4.1), and choosing the polarisation to be a linear combination $a = m + m$ of the left and right circular polarisations, we find the matrix equation

$$\begin{pmatrix} K^2 & \frac{8c}{M^2} \epsilon_{00} \\ \frac{8c}{M^2} \epsilon_{00} & K^2 \end{pmatrix} \begin{pmatrix} 0 \\ 0 \end{pmatrix} = \begin{pmatrix} 0 \\ 0 \end{pmatrix} \quad (4.4)$$

where $K^2 = k^2 + \frac{4b+8c}{M^2} \epsilon_{00}$ and we have used the identity $C_{\mu\nu} m^\mu m^\nu = 0$. The eigenvalues give the modified light cone²

$$k^2 = \frac{4b+8c}{M^2} \epsilon_{00} \pm \frac{8c}{M^2} j_0 j_0 \quad (4.5)$$

This implies a (non-dispersive) polarisation-dependent shift in the speed of light of

$$v = \frac{2b+4c}{M^2} \epsilon_{00} \pm \frac{4c}{M^2} j_0 j_0 \quad (4.6)$$

for the two polarisation eigenstates. We can now show that if we define a phase $\#$ from the (complex) N-P scalar, $\epsilon_{00} = j_0 j_0 e^{i\#}$, then the eigenstates are

$$a = \frac{1}{\sqrt{2}} e^{i\frac{\#}{2}} m \pm e^{-i\frac{\#}{2}} m \quad (4.7)$$

The states which propagate with a well-defined velocity are therefore superpositions of the left and right circular polarisations with equal and opposite phases determined by the Weyl tensor. They are therefore orthogonal linear polarisations, the direction being determined by the Weyl phase.

It should now be reasonably clear that we can equally well apply this formalism to the case of the Lorentz violating phenomenological theory in flat spacetime. (The formal discussion in the remainder of this section and in section 4.2 should be compared with the treatment of photon propagation in refs.[14, 18], where similar issues are addressed without using the Newman-Penrose formalism. The main physics conclusions are the same.) As already noted, the coupling $K_{\mu\nu}$ appearing in the Kostelecky Lagrangian (3.1) plays essentially the same role as the Ricci tensor in the above discussion. In particular, it has the same number of independent components as $R_{\mu\nu}$ by virtue of having the same algebraic symmetries, which are inherited from the operator it multiplies in the Lagrangian. We can therefore introduce the Newman-Penrose formalism in this context also and define N-P scalars $\psi_i^{(K)}$ ($i=0,\dots,4$) from the trace-free analogue $C^{(K)}$ of the Weyl tensor (and similarly for the N-P analogues $\chi_{ij}^{(K)}$ from the traced components $K_{\mu\nu}$). This helps to put some order into the plethora of components of $K_{\mu\nu}$ and extract the essential physics. All the results derived above can now be directly translated. In particular, provided the relevant components of $C^{(K)}$ are non-vanishing, there will be a birefringent velocity shift analogous to eq.(4.6), viz.

$$v = \frac{4}{M^2} \psi_{00}^{(K)} \pm \frac{4}{M^2} j_0 \psi_0^{(K)} j_0 \quad (4.8)$$

²Eq.(4.5) corrects the corresponding equation in ref.[4], where a similar expression was quoted that, although written in terms of ϵ_{00} and $j_0 j_0$, was only valid, and was only used, for the case of real ϵ_{00} .

The velocity eigenstates are given by superpositions of the left and right circular polarisations as in eq.(4.7), where now θ is the phase of $\epsilon_0^{(K)}$. They are therefore orthogonal linear polarisations with orientation determined by θ .

Light with a general linear polarisation is a superposition of these eigenstates. As they propagate through some distance D , the eigenstates will pick up a phase difference $\delta = \frac{2\pi D}{\lambda}$, where λ is the wavelength. The resulting superposition is then no longer a pure linear polarisation, but will be elliptically polarised.³ For a generic orientation of linear polarisation, the major axis of the ellipse will be rotated relative to the direction of linear polarisation by an angle of $O(\lambda)$. The ratio of minor to major axes of the ellipse is also $O(\lambda)$, the exact expressions in each case depending in a non-trivial way on the angle between the polarisation directions of the light wave and the velocity eigenstates. The transformation of linear to elliptic polarisation with a dependence on the propagation distance D is therefore a clear signal for Lorentz breaking through a Weyl mechanism arising from the couplings K in the phenomenological Lagrangian.

A similar analysis also applies to the Chern-Simons interaction in the Lagrangian (3.1). In this case, the appropriate equation of motion is

$$k^2 a - k \cdot a k + i L k \cdot a = 0 \quad (4.9)$$

The modified light cone is derived from

$$\det k^2 g - k \cdot k - i L k = 0 \quad (4.10)$$

which, for physical polarisations, implies [17]

$$k^4 + k^2 L^2 - (L \cdot k)^2 = 0 \quad (4.11)$$

To first order in L , this gives a birefringent phase velocity shift⁴

$$v = \frac{1}{2} \frac{1}{L^2} L \cdot k \quad (4.12)$$

The eigenstates themselves follow from eq.(4.9). As before, choose the physical transverse polarisation vectors to be linear combinations of the left and right circular polarisations, i.e. $a = m + m$. In this sector, the equation of motion becomes

$$\begin{pmatrix} k^2 - i L & m \cdot m k \cdot L \\ 0 & k^2 - i L \end{pmatrix} \begin{pmatrix} m \\ m \end{pmatrix} = \begin{pmatrix} 0 \\ 0 \end{pmatrix} \quad (4.13)$$

³This is the standard situation in optics of superposing two orthogonal plane waves with a phase difference. The resulting figure swept out by the polarisation vector is in general an ellipse, but degenerates to a straight line for special values ($0; \pi/2; \pi; 3\pi/2$) of the phase difference. If the initial two waves have different amplitudes, then the orientation of the principal axes of the ellipse, as well as the ratio of its major to minor axes, depends both on this amplitude ratio as well as on the phase difference. The resulting ellipses are the simplest examples of Lissajous figures. See, for example, ref.[28] for a detailed description.

⁴Notice that, unlike the Weyl case, eq.(4.11) implies a non-trivial dispersion relation. In particular, while the phase velocity satisfies eq.(4.12), the shift in the group velocity is second order in L , i.e. $\frac{\partial v}{\partial k} = 1 + O(L^2)$ [17].

We see immediately, that in contrast to the Weyl case above, the symmetries of the antisymmetric tensor ensure that this matrix is diagonal and therefore the left and right circular polarisations are themselves the eigenstates, i.e. the states which propagate with a well-defined velocity. We can readily check that the light cone condition following from eq.(4.13), viz.

$$k^2 = \frac{1}{2} (k_L^2 + k_R^2) \quad (4.14)$$

reproduces eq.(4.11).

As noted above, linearly polarised light may be considered as a superposition of the left and right circular polarisations with a phase difference which determines the direction of linear polarisation. If the left and right circular polarisations propagate at different speeds, then this phase difference will vary with the distance propagated, thereby rotating the direction of linear polarisation. This birefringent rotation angle is half the induced phase difference between the left and right circular polarisations due to their velocity difference. Linearly polarised light propagating through a distance D will therefore experience a birefringent rotation of the direction of polarisation given by

$$\theta = \frac{2D}{v} \quad (4.15)$$

where v is given by eq.(4.12).

We see, therefore, that there is a distinct difference between the birefringence effects associated with the Weyl (κ) and Chern-Simons (L) types of Lorentz breaking. While the latter simply rotates the direction of linear polarisation, the former in addition turns linear polarisation into elliptic polarisation. Either effect is a clear signal for Lorentz violation; the presence of the latter is characteristic of the parity and CPT violating Chern-Simons interaction.

Clearly, since v is expected to be tiny given that we know Lorentz invariance to be a good symmetry to high accuracy, in order to achieve measurable effects we need the longest possible baseline D , i.e. we need to study deep astrophysical sources emitting linearly polarised radiation for which we can associate a definite direction. We now consider two possible types of source.

4.2 Radio galaxies

A suitable set of astrophysical sources for testing this Lorentz-violation induced birefringence are radio galaxies [17]. These emit synchrotron radiation, which is linearly polarised. Moreover, for a large class of these objects, it is possible to identify an axis along which they are elongated, and models suggest that the alignment of their magnetic field determines the orientation of the emitted linear polarisation to be either along, or orthogonal to, this axis.

Carroll, Field and Jackiw [17] have carried out a detailed study of a sample of 160 such radio galaxies, with redshifts typically in the range $z = 0.1$ to $z = 1$. Making cuts to those with polarisations above 5% and with $z > 0.4$, and after compensating for the effects of Faraday rotation by the intergalactic magnetised plasma, they find clear evidence that the observed orientation of the linear polarisation is indeed peaked around 90° relative to the

axis of the radio galaxy. The mean angle is found to be $90.4^\circ \pm 3.0^\circ$. They conclude that at the 95% confidence level, the birefringent rotation angle implied by a Chern-Simons mechanism is $\alpha < 6.0^\circ$.

To convert this into a bound for the Chern-Simons coupling, we need to convert from the redshift to the proper distance D . For an $\Omega_m = 1$ matter dominated universe, this gives $D = \frac{2}{3H_0} (1+z)^{\frac{3}{2}}$, where H_0 is the Hubble constant. Letting $h = H_0/100 \text{ km sec}^{-1} \text{ Mpc}^{-1}$, the recent WMAP data[29] determines $h = 0.72 \pm 0.05$. It follows from eqs.(4.12), (4.15) that

$$= \frac{1}{2} D L \hat{k} \quad (4.16)$$

$$= \frac{1}{3H_0} (1+z)^{\frac{3}{2}} L \hat{k} \quad (4.17)$$

from which, taking $z = 0.4$, we deduce the following bound on the Chern-Simons coupling[17]

$$|L \hat{k}| < 1.2 \times 10^{-42} \text{ GeV} \quad (4.18)$$

Alternatively, from the discussion following eq.(4.8), we can use the observation of linear (rather than elliptic) polarisation, with the predicted orientation, to estimate a bound for the dimensionless Weyl coupling $\kappa_0^{(K)}$ obtained from the couplings K in the phenomenological Lagrangian (3.1). With the above bound on $L \hat{k}$, and a typical radio galaxy wavelength of $\lambda = 20 \text{ cm}$, we can use eq.(4.15) together with (4.8) to obtain the following estimate:

$$|\kappa_0^{(K)}| < 0.10 \times 10^{-29} \quad (4.19)$$

Notice that because of the qualitatively different dispersion relations for the Weyl and Chern-Simons mechanisms, i.e. $v = \text{const}$ for Weyl (eq.(4.8)) and $v = 1/k$ for Chern-Simons (eq.(4.12)), the birefringent rotation angle $\alpha = D v$ is independent of the frequency of the radiation for Chern-Simons but is proportional to frequency for the Weyl case, as used above.⁵ It follows that in order to bound the Weyl coupling, we can look not only for sources with long baselines D , but also study them at shorter wavelengths.

Taking advantage of this, a more recent estimate has been made by Kostelecky and Mewes[18] using a smaller sample of higher redshift galaxies and quasars for which polarimetric measurements are available in the infra-red, optical and UV. From this, they are able to quote an improved bound of $O(10^{-32})$ on a typical component of K .

4.3 Gamma-ray bursts

As noted above, one way to improve these bounds is to increase the baseline distance D by studying polarisation in astrophysical sources at higher redshifts, while for some couplings, observing sources at higher frequencies will also help. An intriguing new possibility in this

⁵ It should be noted, however, that the constant dispersion relation in the Weyl case is a consequence of only retaining the renormalisable $\text{dim} = 4$ operator in the extended QED Lagrangian. In the general case where higher-dimensional operators are considered as well, as in the strong equivalence violating Lagrangian in section 2, the corresponding dispersion relation is highly non-trivial[6].

direction has been opened up in the last few years by the detection of linear polarisation in gamma-ray burst (GRB) afterglows, i.e. the fading optical phase observed after the initial prompt burst of gamma-rays, and recently in the prompt gamma-ray phase itself.

The first observation of polarisation in GRB afterglows was made in 1999 in GRB 990123, which has a redshift of $z = 1.60$. Since then, around ten further observations have been made. (See ref.[30] for a complete list.) Amongst these, the highest redshift recorded so far is $z = 2.33$, for GRB 021004.

It is very likely that in the next few years increasingly precise observations of GRBs, notably with the forthcoming launch of the SWIFT satellite, will substantially increase the data set of observations of polarisation in GRB afterglows. Eventually we may hope that polarisation measurements on GRBs will evolve from their present role as probes of the basic mechanism of GRB production to tools which we can exploit to constrain the fundamental physics of light propagation. If GRB polarisation does indeed come to be as well understood as the polarisation from radio galaxies discussed above, the increase in redshift by a factor of around 10 will allow us to tighten the bounds (4.18), (4.19) still further.

In order to realise this programme, we need first of all to observe intrinsic linear polarisation in high redshift GRBs, and also to understand its direction in terms of the geometry of the source/observer so that we can place bounds on any birefringent rotation. We also need to understand the effect on polarisation of the transmission of the afterglow light through the host galaxy (see e.g. refs.[31, 32], a challenging task analogous to the subtraction of Faraday rotation in the intergalactic medium in the analysis of polarisation with radio galaxies. It will clearly be some time before all this can be achieved, but our purpose in this section is simply to draw attention to the possibility of using GRBs as controlled long-baseline light sources for the study of fundamental physics such as the possible violation of Lorentz invariance.

As an illustration of how directed, linear polarisation can arise in GRB afterglows⁶, we consider a simple model proposed by Ghisellini and Lazzati[33]. Several other models can be found in the literature, which differ in important respects and should be readily distinguishable as more data becomes available.⁷ The key features in many cases though are common: (i) GRBs arise through the ejection of a jet of relativistic matter in a narrow cone from a central source, almost certainly a supernova. This jet structure removes spherical symmetry and provides the essential axis for the source analogous to the elongation direction of the radio galaxies. (ii) Synchrotron radiation is emitted from the relativistic electrons accelerated in the magnetic field of this jet, with the radiation emitted at 90°

⁶In what follows, we are describing a mechanism for polarisation in GRB afterglows, where it seems to be accepted that the relevant production mechanism is synchrotron radiation. Polarisation of the prompt gamma-rays in a GRB has recently been observed in GRB 021206. Here, authors appear divided on whether the origin is synchrotron radiation or inverse Compton scattering. See ref.[32] for a brief summary.

⁷We do not enter here into the comparison of models, which differ in such important features as whether the magnetic field in the jet of ejected matter is completely tangled or partially ordered, whether the jet is homogeneous or structured, and whether or not the jet cone opening angle is itself sufficiently small that only the angle to the observer's line of sight is relevant. See, for example, refs.[34, 32] for an introduction to the literature.

being linearly polarised. (iii) This synchrotron radiation is Lorentz boosted by the usual relativistic aberration mechanism into the forward direction where it can be received by the observer. (iv) Crucially, observations are made off the axis of the jet cone. This introduces the asymmetry necessary to observe a non-vanishing net polarisation.

Consider then a shell of magnetised plasma moving outwards relativistically in a jet making a cone of half-angle θ_c . Synchrotron radiation is emitted from the shell with the radiation emitted in its plane, i.e. at 90° to the outward motion, being linearly polarised. This jet is observed off-axis by an observer whose line of sight makes an angle θ_o with the jet axis. See Figure 1.

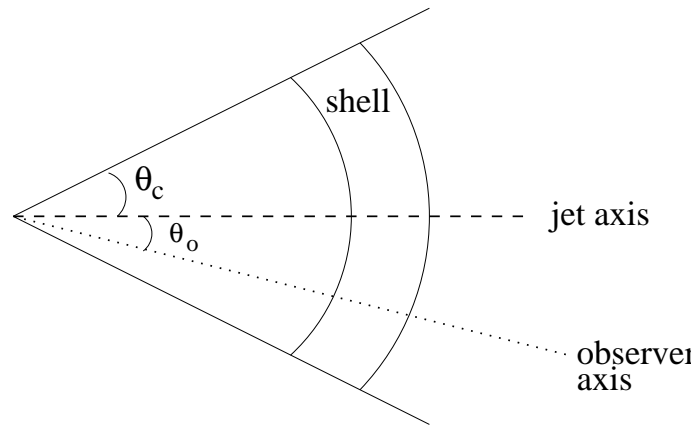


Figure 1: A jet comprising a shell of magnetised plasma is emitted radially outwards forming a cone of half-angle θ_c . It is observed off-axis by an observer whose line of sight makes an angle θ_o with the jet axis.

Because of relativistic aberration, photons emitted in the plane of a segment of the shell, in its comoving frame, are observed in the forward direction making an angle $\theta = 1/\gamma$ with the normal, where γ is the Lorentz factor. See Figure 2. This means that the observer

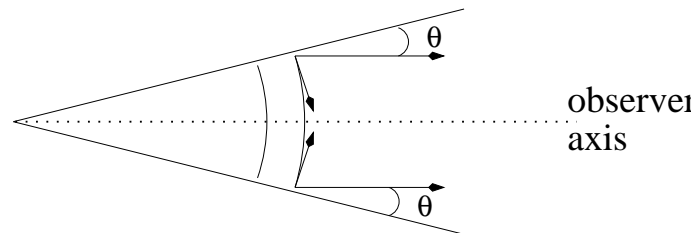


Figure 2: Polarised light emitted at right angles to the outward radial motion of a section of the plasma shell is relativistically aberrated into the forward direction, where it makes an angle $\theta = 1/\gamma$ with the normal to the shell. It is observed at the edge of the circle subtending a cone of half-angle θ_o about the observer's line of sight axis.

receives linearly polarised light from the edge of the circle subtending a cone of half-angle θ_o around the line of sight. The polarisation direction is radial with respect to this circle.

If the observer's cone lies entirely within the jet cone, then this whole circle is observed and the net polarisation is zero through cancellation of the radially-directed polarisation

around the circle. As γ increases, however, only a part of the observer's cone overlaps with the jet cone. In this case, only part of the circle is observed and a net polarisation is measured. See Figure 3. Finally, as γ increases still further, the observer's cone completely envelopes the jet cone and again no polarisation is observed.

The criterion for observing a net linear polarisation is therefore

$$\frac{1}{\gamma + \beta} > \frac{1}{\gamma - \beta} \quad (4.20)$$

that is,

$$\frac{1}{\gamma + \beta} < \frac{1}{\gamma - \beta} \quad (4.21)$$

Notice that this is only possible if $\beta \neq 0$, i.e. if the GRB jet is viewed off-axis.

To summarise, at the beginning of the afterglow when γ is large, the observer sees only a fraction of the full jet ($\gamma > 1 = \gamma_{\text{c}} = \gamma_0$) and no net polarisation is observed. As γ drops as the afterglow evolves, we enter the asymmetric stage where the observer's cone overlaps partly with the jet cone (this results in an observed net polarisation). As γ falls still further ($\gamma < 1 = \gamma_{\text{c}} + \gamma_0$), the entire jet cone becomes visible and the polarisation vanishes.

This model also makes a definite prediction for the direction of polarisation. The derivation is given in detail in ref.[33] and consists of integrating the Stokes' vectors Q and U around the visible arc of the observer's circle. The result, which is a peculiarity of this precise geometric model, is that the polarisation is initially orthogonal to the plane containing both the jet cone axis and the line of sight, before flipping abruptly to lie in this plane. All models of this type, however, make a well-defined prediction of the direction of polarisation.

For our purposes, the crucial point to be extracted from this model is that we should expect to observe a net linear polarisation, with a specified direction established with respect to the plane formed by the jet axis and the observer's line of sight, in a situation where a GRB jet is observed off-axis (as will generically be the case). The existence, and possibly direction, of this linear polarisation is expected to change with time as the Lorentz factor γ reduces as the expanding jet slows.

GRB afterglows therefore satisfy the criteria we need for the long-baseline astrophysical polarimetry measurements which can test Lorentz and CPT symmetry to high accuracy. Moreover, if polarisation measurements meeting these criteria can eventually also be made on the prompt gamma-rays themselves, we could also improve the bounds on the Weyl' coupling because of the extremely small wavelength factor in the birefringent rotation formula, as discussed above.

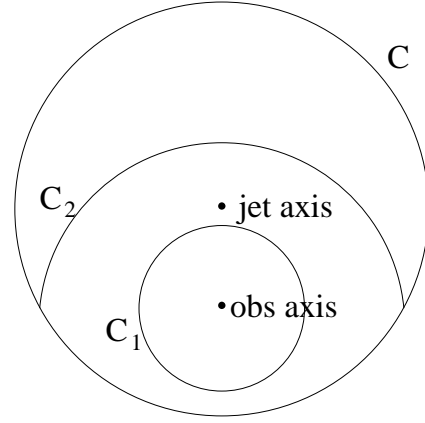


Figure 3: The circle C subtends the jet cone. Circles C_1 and C_2 subtend the observer's cone of half-angle $1 = \gamma$ as γ increases. Initially C_1 lies entirely within C , while for lower values of the Lorentz factor there is only a partial overlap, enabling a net linear polarisation to be observed.

This combination of large redshifts and high frequencies means that GRBs have the potential ultimately to give the most accurate limits on the Lorentz and CPT violating couplings $j^{(K)}$ and \tilde{j}_j .

5. Precision Atomic Spectroscopy

While testing the Maxwell sector of the Lorentz and CPT violating theory requires observations on astronomical scales, testing the Dirac sector is the domain of precision atomic physics experiments. In this section, we will consider the implications of the phenomenological Lagrangian (3.1) for precision atomic spectroscopy, in particular with hydrogen and antihydrogen. The possibility of making spectroscopic experiments on antihydrogen and looking for CPT violation follows from the production for the first time of substantial numbers of cold antihydrogen atoms at the ATHENA [20, 21] and ATRAP [22, 23] experiments at CERN in 2002. This subject has already been investigated in detail by Bluhm, Kostelecky and Russell [24], but here we shall push their analysis a little further to see whether there are further options for CPT tests which could be realised at ATHENA and ATRAP.

5.1 Hydrogen spectrum with Lorentz and CPT violation

Our starting point is the textbook derivation of the relativistic fine structure of hydrogen energy levels starting from the Dirac equation, rather than the more familiar derivation based on perturbation theory and the non-relativistic Schrodinger equation. In outline, this derivation goes as follows. The non-relativistic Schrodinger equation for hydrogen reduces to

$$\frac{1}{2m} \frac{\partial^2}{\partial r^2} + \frac{2}{r} \frac{\partial}{\partial r} - \frac{L^2}{r^2} - \frac{E_n}{r} \psi_n(\mathbf{r}) = 0 \quad (5.1)$$

where the wave function $\psi_n = \exp(-iEt) \psi_n(\mathbf{r})$, $L^2 \psi_n = \ell(\ell+1) \psi_n$, and the energy eigenvalues are $E_n = -\frac{1}{2} m \alpha^2 = -n^2$, where the integer n satisfies $\ell = 0; 1; \dots; n-1$.

We now reduce the full QED field theory to one-particle relativistic quantum mechanics in the usual way, regarding the Dirac equation as a relativistic wave operator, in a classical background A-field, acting on a four-component wave function ψ , i.e.

$$i \not{D} \psi - m \psi = 0 \quad (5.2)$$

where $\not{D} = \not{\partial} + ie \not{A}$. Now act on this with the Dirac operator with $m \rightarrow -m$. This gives

$$D^2 \psi - e \not{F} \psi - m^2 \psi = 0 \quad (5.3)$$

Substituting the Coulomb potential $eA_0 = -\frac{1}{r}$, $A_i = 0$, and using the explicit expressions for the matrices⁸, this becomes

$$\frac{\partial^2}{\partial r^2} + \frac{2}{r} \frac{\partial}{\partial r} - \frac{L^2}{r^2} + \frac{1}{r} + 2E \frac{1}{r} + E^2 - m^2 - \frac{i}{r^2} \frac{\partial}{\partial \theta} \left(\frac{\partial}{\partial \theta} \right) = 0 \quad (5.4)$$

⁸Our conventions for the matrices are:

$$\gamma_0 = \begin{pmatrix} 0 & 1 \\ 1 & 0 \end{pmatrix}, \quad \gamma_i = \begin{pmatrix} 0 & \sigma_i \\ \sigma_i & 0 \end{pmatrix}, \quad \gamma_5 = \begin{pmatrix} 1 & 0 \\ 0 & -1 \end{pmatrix}$$

which separates into two almost identical equations for the two-component spinor wave functions in the decomposition $\psi = \psi^+ + \psi^-$, viz.

$$\frac{\partial^2}{\partial r^2} + \frac{2}{r} \frac{\partial}{\partial r} - \frac{n^2}{L^2} - 2 \left(1 - \frac{1}{r} \right) + 2E \frac{1}{r} + E^2 - m^2 = 0 \quad (5.5)$$

We can show [35] that the eigenvalues of the operator $\frac{n^2}{L^2}$ can be written as $-(j+1)$ where $j = [(j+\frac{1}{2})^2 - \frac{1}{4}]^{\frac{1}{2}}$; $[(j+\frac{1}{2})^2 - \frac{1}{4}]^{\frac{1}{2}} - 1$ for $j = \frac{1}{2}, \frac{3}{2}$ respectively. In each case, this gives $j = \frac{1}{2}$ where $j = \frac{1}{2j+1} + O(\frac{1}{j^4})$.

Now, comparing eq.(5.5) with the non-relativistic Schrodinger equation (5.1), we deduce by inspection that the energy eigenvalues in the relativistic equation satisfy

$$E^2 - m^2 = \frac{1}{(n-j)^2} (E - m)^2 \quad (5.6)$$

Expanding in powers of $1/n$, we recover the familiar expression for the fine-structure correction to the hydrogen energy levels in the relativistic theory:

$$E_{FS} = m \left[1 - \frac{1}{2} \frac{m^2}{n^2} + \frac{1}{2} \frac{m^4}{n^3} \left(\frac{3}{4n} - \frac{1}{j+\frac{1}{2}} \right) + O\left(\frac{1}{n^6}\right) \right] \quad (5.7)$$

We now consider the implications of changing the Dirac equation to the extended one implied by the Lorentz-violating Lagrangian (3.1), viz.

$$i \not{D} \psi - m \psi - a \not{b}^5 + i c \not{D} + i d \not{b}^5 \not{D} - \frac{1}{2} h \not{D}^2 = 0 \quad (5.8)$$

Multiplying as before by the equivalent operator with $m \rightarrow -m$, we find that the extended Dirac one-particle relativistic wave equation analogous to eq.(5.3) is

$$\not{D}^2 \psi - e \not{F} \psi - m^2 \psi - 2ia \not{D} - 4b \not{b}^5 \not{D} - c \not{D} - 2D \not{D} - ie \not{F} - 2e \not{F} \not{D} - d \not{b}^5 - 4i \not{D} \not{D} - ie \not{F} - 2e \not{F} + \frac{1}{2} h \not{D}^2 = 0 \quad (5.9)$$

To see the effect of the new Lorentz and CPT violating couplings, consider first just adding the a and b terms. Using the explicit expressions for the γ matrices, we find, to

where σ_i are the Pauli matrices, and

$$\gamma_5 = \frac{i}{4} \epsilon_{ijk} \gamma_i \gamma_j \gamma_k$$

which implies

$$\gamma_0 \gamma_i = \frac{i}{2} \epsilon_{ijk} \gamma_j \gamma_k \quad \gamma_i \gamma_j = \frac{1}{2} \epsilon_{ijk} \gamma_k \gamma_0$$

We also need the following identity in the derivation of eq.(5.4):

$$\gamma_i \gamma_j = -\delta_{ij} + \epsilon_{ijk} \gamma_k \gamma_5$$

rst order in the small couplings a ; b :

$$\begin{aligned} \frac{\partial^2}{\partial r^2} + \frac{2}{r} \frac{\partial}{\partial r} - \frac{L^2}{r^2} + \frac{1}{r} + 2E \frac{1}{r} + E^2 - m^2 - \frac{1}{r^2} \left(\frac{1}{0} - \frac{1}{0} \right) \\ + 2E a_0 + 2a_0 \frac{1}{r} - \frac{1}{2} E \frac{b_0}{r} - \frac{1}{2} \frac{1}{r} \frac{b_0}{r} + O(r^{-1}) = 0 \end{aligned} \quad (5.10)$$

We now come to the key step. Comparing eqs.(5.4) and (5.10), we see by inspection that to rst order in the couplings, the energy eigenvalues are simply related by

$$E = E_{FS} + a_0 - \frac{1}{4} \frac{b_0}{r} \quad (5.11)$$

That is, introducing the spin operator $\underline{S} = \frac{1}{2} \underline{\sigma}$, the energy eigenvalues in the Lorentz violating theory are

$$E = E_{FS} + a_0 - \frac{1}{2} \hbar b_0 \underline{S} \cdot \underline{i} \quad (5.12)$$

Extending the analysis to include the remaining couplings, we readily find the complete result

$$E = E_{FS} + (a_0 + m c_{00}) - \frac{1}{2} (b_i - m d_{i0} + \epsilon_{ijk} h^{jk}) \hbar S^i \cdot i \quad (5.13)$$

To complete the derivation, we need the matrix element $\hbar S^i \cdot i$ taken in the basis of states $|j, m_j\rangle$ appropriate for the structure.⁹ In fact, this is well-known from the perturbative analysis of the Zeeman effect. The result is

$$\langle j, m_j | S_z | j, m_j \rangle = g m_j \quad (5.14)$$

⁹The evaluation of the matrix element of the spin operator $\hbar S_i$ in $|j, m_j\rangle$ proceeds as follows. Abbreviate the notation $|j, m_j\rangle$ to $|j, m\rangle$. From the definition of the Clebsch-Gordon coefficients,

$$|j, m\rangle = \sum_{m_1, m_2} \langle j_1, m_1; j_2, m_2 | j, m \rangle |j_1, m_1\rangle |j_2, m_2\rangle$$

we readily find

$$\langle j, m | S_z | j, m \rangle = \sum_{m_1, m_2} \langle j_1, m_1; j_2, m_2 | j, m \rangle \langle j_1, m_1 | S_z | j_1, m_1 \rangle \langle j_2, m_2 | j, m \rangle$$

while

$$\langle j, m | S_{\pm} | j, m \rangle = \sum_{m_1, m_2} \langle j_1, m_1; j_2, m_2 | j, m \rangle \langle j_1, m_1 | S_{\pm} | j_1, m_1 \pm 1 \rangle \langle j_2, m_2 | j, m \rangle$$

For $s = \frac{1}{2}$, and using the known expressions for the Clebsch-Gordon coefficients[36], we then find for $m_j = m$ and the two possibilities $j = \frac{1}{2}$,

$$\begin{aligned} \langle j, m | S_z | j, m \rangle &= \frac{1}{2} m \\ \langle j, m | S_{\pm} | j, m \rangle &= \frac{1}{2} \sqrt{s(s+1) \mp m} \end{aligned}$$

while $\langle j, m | S_{\pm} | j, m \rangle = 0$. The diagonal matrix element is the result quoted above.

where g is the Lande g -factor,

$$g = \frac{1}{2j(j+1)} [j(j+1) + s(s+1) - \ell(\ell+1)] \quad (5.15)$$

while $h S_z = 0$. For $s = \frac{1}{2}$,

$$h n \langle s_j m_j | S_z | j m_j \rangle = \frac{1}{2\ell+1} m_j \quad (5.16)$$

for the two possibilities $j = \ell \pm \frac{1}{2}$. Putting all this together, we finally find the following result for the energy eigenvalues for hydrogen in the Lorentz and CPT violating phenomenological theory (3.1):

$$E = E_{FS} + (a_0 + m c_0) - \frac{1}{2} (b_3 - m d_{30} + h_{12}) \left(\frac{1}{2\ell+1} \right) m_j \quad (5.17)$$

for $j = \ell \pm \frac{1}{2}$.

The important new feature here compared with the result quoted in ref.[24], which was concerned purely with the $1s \rightarrow 2s$ transition involving only $\ell = 0$ states, is the ℓ -dependence in the general case arising from the Lande g -factor.

Notice also that since the contribution of the a and c couplings to the energy levels is independent of the angular momentum and spin quantum numbers, they do not affect energy differences between states so play no role in determining the transition frequencies. The couplings which do have the potential to change the transition frequencies are b , d and h . These are the parity-violating couplings which did not have analogues in the strong equivalence violating QED Lagrangian discussed earlier (see the dictionary in eq.(3.2).) In order to have curvature-induced effects on atomic spectra, we would need to go beyond the extended QED model of section 2, either by introducing parity-violating couplings on a purely ad-hoc basis into the phenomenological Lagrangian or by embedding QED in an extended strong equivalence violating standard model with electroweak parity violation.

5.2 $1s \rightarrow 2s$ and $2s \rightarrow nd$ ($n \geq 10$) transitions in H and anti-H

In order to test for Lorentz and CPT violation in atomic spectroscopy, at least in the context of this model, we need to compare transition frequencies which are sensitive to the couplings b_3, d_{30} and h_{12} . One promising approach is to compare the frequencies of the equivalent spectral lines in hydrogen and anti-hydrogen, now that the abundant production of cold anti-hydrogen atoms at ATHENA [20, 21] and ATRAP [22, 23] has made precision spectroscopy on anti-hydrogen feasible for the first time.

As noted in section 3, the couplings change in the following way under charge conjugation: $a \rightarrow a, b \rightarrow b, c \rightarrow c, d \rightarrow d, h \rightarrow h$. Transition frequencies sensitive to the combination $(b_3 - m d_{30} + h_{12})$ will therefore be different for hydrogen and anti-hydrogen. Measuring such a difference in their spectra would be a clear signal for Lorentz, and possibly CPT, invariance.

So far, attention has focused on the $1s \rightarrow 2s$ transition. This is a Doppler-free, two-photon transition: two-photon since it violates the usual single-photon, electric-dipole

selection rule $\lambda = 1$ and Doppler-free since the recoil momentum from the emission of the two photons cancels. The $2s$ state is therefore exceptionally long-lived (lifetime 122ms) and the $1s \rightarrow 2s$ spectral line has an ultra-narrow natural linewidth of 1.3Hz, giving a resolution of $O(10^{-15})$. ($\lambda = 243\text{nm}$ for the two-photon $1s \rightarrow 2s$ transition.) It has been suggested that an even more accurate measurement of the line centre to 1mHz, corresponding to an ultimate resolution of one part in 10^{18} , is in principle attainable [37, 38]. The $1s \rightarrow 2s$ transition is therefore favoured for precision spectroscopy.

The selection rules for two-photon transitions are derived in ref.[39]. The principle is straightforward. The transition amplitude depends on the product of two vector dipole operators, which is decomposed as the sum $(T_q^0 + T_q^2)$ of scalar and rank-two irreducible tensor operators, where the quantum numbers q are correlated with the helicities of the emitted photons. For the special case of $\lambda = 0$ to $\lambda = 0$ transitions, only the scalar operator T_q^0 can couple the two states and the resulting selection rule is

$$j = 0; \quad m_j = 0 \quad (\lambda = 0 \rightarrow \lambda = 0) \quad (5.18)$$

Applied to the $1s \rightarrow 2s$ transition, the important fact for us is the constraint $m_j = 0$. According to eq.(5.17), the $1s$ and $2s$ energy levels receive the same corrections if they have the same m_j . The selection rule $m_j = 0$ therefore ensures that the $1s \rightarrow 2s$ transition frequency is unchanged by the Lorentz and CPT violating couplings.

To overcome this problem, Bluhm, Kostelecky and Russell [24] have made a detailed study of the $1s \rightarrow 2s$ hyperfine transitions for hydrogen and anti-hydrogen. We shall only briefly summarise some of their results here; see ref.[24] for full details. In particular, they exploit the n -dependence of the hyperfine splitting for a certain spin-mixed state to show that the corresponding $1s \rightarrow 2s$ hyperfine transition receives a frequency shift due to the Lorentz and CPT violating couplings of

$$H \quad b_3^e \quad b_3^p \quad m_e d_{30}^e + m_p d_{30}^p \quad h_{12}^e + h_{12}^p \quad (5.19)$$

where θ is a combination of magnetic field dependent mixing angles. Notice that we have included the corresponding couplings for a modified Dirac equation for the proton as well as the electron in eq.(5.19). Since the corresponding hyperfine states in anti-hydrogen have the opposite spin assignments to hydrogen, the result in this case is

$$H \quad b_3^e + b_3^p \quad m_e d_{30}^e + m_p d_{30}^p \quad h_{12}^e + h_{12}^p \quad (5.20)$$

An observation of this hyperfine transition in hydrogen would therefore exhibit sidereal variations because of the frame dependence implicit in the Lorentz violating couplings. Moreover, if we could compare with the equivalent transition in anti-hydrogen, there would be an instantaneous difference

$$H \quad H \quad 2 \quad b_3^e \quad b_3^p \quad (5.21)$$

This would provide a direct measurement of the CPT-odd coupling b_3 . A positive observation would therefore be a signal of the violation of CPT symmetry. If θ could be

measured with an accuracy comparable to the ultimate line centre of 1mHz, this would place a bound of $b_j < 10^{-27} \text{GeV}$ on the CPT-violating coupling¹⁰.

The magnetic field needed to resolve the hyperfine states is naturally present because cold anti-hydrogen is produced in magnetic fields in the ATHENA and ATRAP experiments and it is likely that spectroscopic measurements will be made on anti-hydrogen atoms confined in a magnetic trap. (For details, see e.g. ref.[42].) However, the inhomogeneous nature of the trapping fields produces Zeeman broadening of the spectral lines and limits the resolution that can actually be achieved in practice. It is estimated in ref.[24] that this could broaden the 1s–2s hyperfine spectral line described above to over 1MHz width, which corresponds to an actual experimental resolution of only one part in 10^9 . In ref.[38], the possibility of achieving a width of 20kHz is envisaged. Reducing Zeeman broadening and developing techniques to determine the line centre to even higher accuracy in order to approach the theoretically limiting resolution of the 1s–2s transition is therefore an important experimental challenge[42].

In the remainder of this section, we will investigate an alternative to 1s–2s for precision studies of Lorentz and CPT violation, exploiting the ℓ -dependence in the Lande g-factor in the formula (5.17) for hydrogen energy levels. Of particular interest is the Doppler-free, two-photon 2s–nd transition for $n \geq 10$. This turns out to be surprisingly competitive with the 1s–2s transition for practical precision spectroscopy. Indeed, at the time of writing of the comprehensive review of hydrogen spectroscopy ref.[43], the 2s–8;10;12d transitions provided the most accurate determination of the Rydberg constant, to one part in 10^{10} [44]. In fact, the limitation on further improvement comes not from the natural width of the spectral lines but from the accuracy of the optical laser frequencies. The 2s–10d natural linewidth is 296kHz while the experimental linewidth reported in ref.[45] is 1.25MHz.

It seems possible, therefore, that in realistic experimental conditions, measurements of the 2s–nd ($n \geq 10$) transition in free hydrogen and anti-hydrogen (see ref.[46] for ‘atomic fountain’ techniques to study free cold atoms outside magnetic traps) could be made with a high precision complementing the 1s–2s hyperfine Zeeman transition¹¹. The loss of accuracy due to the broader natural linewidth of 2s–nd is compensated by the absence of the Zeeman broadening which affects the 1s–2s hyperfine transition, in addition to a variety of other experimental limitations including the accuracy of the laser frequencies at the required wavelengths. Naturally, though, a much more detailed experimental analysis would be required to confirm whether or not the 2s–nd transition is really competitive, especially in the case of anti-hydrogen.

Our interest in the 2s–nd transition stems of course from the fact that invoking an $\ell = 2$ state allows us to exploit the ℓ -dependence in the energy level formula (5.17). While the 2s state has only $j = \frac{1}{2}$; $m_j = \pm \frac{1}{2}$ quantum numbers, the nd state allows

¹⁰A compilation of similar bounds from a variety of atomic physics experiments is given in ref.[40]. See also ref.[41] for a review invoking a broader range of Lorentz violating models.

¹¹The case $n = 11$ may be of particular interest in the ATHENA programme as anti-hydrogen atoms in this state will be produced using appropriate laser frequencies to induce transitions from the high n Rydberg states in which they are originally formed.

$j = \frac{3}{2}; m_j = \frac{3}{2}; \frac{1}{2}$ and $j = \frac{5}{2}; m_j = \frac{5}{2}; \frac{3}{2}; \frac{1}{2}$. Eq.(5.17) therefore predicts a non-zero contribution from the Lorentz and CPT violating couplings at the level of the basic spectral line, without needing to introduce a magnetic field to produce hyperfine Zeeman splittings.

The selection rules for $2s \rightarrow 1s$ are as follows. For $\lambda \neq 0$, the scalar operator T_q^0 gives no contribution, so the selection rules follow from the two-photon matrix elements of the rank-two tensor operator T_q^2 . The selection rules for the $\lambda = 2$ transition are [39]

$$j_1 j_2 \rightarrow j; \quad m_j = q_1 + q_2 \quad (\lambda = 2) \quad (5.22)$$

where q_1, q_2 are the photon helicities. Transitions between nearly all the $j; m_j$ states above are therefore possible, with the only restriction $j m_j \rightarrow j \pm 2$.

The frequency shift induced by the new couplings is therefore¹²

$$= \frac{1}{2} (b_3 - m d_{30} + h_{12}) \left(\frac{1}{5} m_j^{nd} - m_j^{2s} \right) \quad (5.23)$$

where the $\frac{1}{5}$ refers to $j = \frac{5}{2}$ and $\frac{3}{2}$ respectively. Exploiting this dependence on the quantum numbers, successive measurements on hydrogen alone can therefore determine the combination $(b_3 - m d_{30} + h_{12})$. In addition, there will be sidereal variations due to the frame dependence associated with Lorentz violation.

The same measurements on anti-hydrogen would determine the charge conjugate contribution $(b_3 + m d_{30} - h_{12})$. Comparing the hydrogen and anti-hydrogen results therefore enables us to make an independent determination of the CPT-violating coupling b_3 and the Lorentz-violating, but CPT-preserving, combination $m d_{30} - h_{12}$.

In conclusion, the transition $2s \rightarrow 1s$ in free hydrogen and anti-hydrogen allows us to exploit in full the quantum number dependence of the general energy level formula (5.17). In realistic experimental conditions, taking account of issues such as Zeeman broadening in the magnetic trap required to study the hyperfine Zeeman $1s \rightarrow 2s$ transition and the limitations from laser frequency accuracy at the relevant wavelengths, it may even prove comparable in resolution with the $1s \rightarrow 2s$ transition. In any case, it provides an interesting complementary measurement in anti-hydrogen spectroscopy.

6. Conclusions

In this paper, we have investigated the construction and experimental implications of phenomenological extensions of QED exhibiting violations of the strong equivalence principle, Lorentz invariance or CPT symmetry. The underlying theme has been the formal similarity between these models. Both are essentially theories of the phenomenology of Lorentz non-invariant operators. In Kostelecky's Lorentz-violating model, these operators arise with multi-index couplings (perhaps to be interpreted as VEVs of tensor operators in a more fundamental theory of spontaneous Lorentz symmetry breaking), which may be bounded by experiment. In the strong equivalence violating models, this role is played by the curvature tensors of the background gravitational field.

¹²For simplicity of presentation, we are neglecting the effect of the nuclear proton spin here.

Modifications to the Maxwell sector of QED can be tested to high accuracy using long-baseline polarimetry observations of astrophysical sources. After reviewing existing limits on birefringent propagation obtained from radio galaxies and quasars, we have shown how in future polarisation measurements on gamma-ray bursts at high redshift have the potential to enable even more stringent bounds to be placed on the Lorentz-violating Maxwell couplings K and L .

In the Dirac sector, experimental tests of Lorentz and CPT violation can be made with high precision atomic spectroscopy comparing hydrogen and antihydrogen, the latter having become feasible following the recent production of cold antihydrogen atoms in significant numbers by the ATHENA and ATRAP collaborations. On the basis of an extended formula for atomic energy levels, we have proposed that the transition $2s \rightarrow 1s$ in free hydrogen and antihydrogen may provide a useful complement to the currently envisaged programme of spectroscopy on the $1s \rightarrow 2s$ hyperfine Zeeman transition.

One of the original motivations for this paper was to investigate whether the constraints on these models obtained from astrophysics could be used to bound the couplings giving rise to Lorentz and CPT violation in atomic spectroscopy, and vice-versa. At first sight, it appears that, in particular, the Chern-Simons photon coupling L and the CPT-violating electron coupling b should be related through radiative corrections. If so, this would have important implications for the atomic physics experiments since, as we have seen, the existing bounds from radio galaxies constrain $|L| < O(10^{-42}) \text{ GeV}$ while, even under the most optimistic experimental scenario, antihydrogen spectroscopy can only reach a bound of $|b| < O(10^{-27}) \text{ GeV}$. However, ambiguities in the specification of the quantum theory based on the Kostelecký Lagrangian arising from the axial anomaly make the relation between b and L strictly indeterminate, though perhaps it could still be argued that we would naturally expect them to be of the same order of magnitude. On the other hand, where the relation between couplings is free of anomaly ambiguities, as we would expect to be the case with a_μ , c and K , the Dirac couplings do not affect the frequency of atomic transitions.

The strong equivalence principle, Lorentz invariance and CPT symmetry are all fundamental ingredients of conventional quantum field theories of elementary particle physics and cosmology. Nevertheless, as we have seen, it is relatively straightforward to modify the dynamics of QED or the standard model to exhibit violations of each of these principles and to predict corresponding experimental signatures, either in atomic physics or astronomy. Hopefully, these theoretical considerations will help to stimulate further high-precision experimental work to test their validity to still greater accuracy.

Acknowledgements

I would like to thank M. Charlton and D. P. van der Werf for interesting discussions.

References

- [1] I.T. Drummond and S. Hathrell, Phys. Rev. D 22 (1980) 343.
- [2] R.D. Daniels and G.M. Shore, Nucl. Phys. B 425 (1994) 634.
- [3] R.D. Daniels and G.M. Shore, Phys. Lett. B 367 (1996) 75.
- [4] G.M. Shore, Nucl. Phys. B 460 (1996) 379.
- [5] G.M. Shore, Nucl. Phys. B 605 (2001) 455.
- [6] G.M. Shore, Nucl. Phys. B 633 (2002) 271.
- [7] G.M. Shore, Superluminal Light, to appear in the Proceedings: Time and Matter: An International Colloquium on the Science of Time', Venice 2002, eds. I. Bigi and M. Faessler, gr-qc/0302116.
- [8] G.M. Shore, Nucl. Phys. B 646 (2002) 281.
- [9] M.A. Leontovich, in L.I. Mandelstam, Lectures in Optics, Relativity and Quantum Mechanics, Nauka, Moscow 1972 (in Russian).
- [10] Y. Ohkuwa, Prog. Theor. Phys. 65 (1981) 1058.
- [11] F.A. Berends and R. Gastmans, Annals of Physics 98 (1976) 225.
- [12] K.A. Milton, Phys. Rev. D 15 (1977) 538.
- [13] J.F. Donoghue, B.R. Holstein, B. Garbrecht and T. Konstandin, Phys. Lett. B 529 (2002) 132.
- [14] D. Colladay and V.A. Kostelecky, Phys. Rev. D 55 (1997) 6760; D 58 (1998) 116002.
- [15] V.A. Kostelecky, in Proc. Intl. Conf. Orbis Scientiae 2000, Coral Gables, Dec. 2000.
- [16] S. Weinberg, The Quantum Theory of Fields, Cambridge University Press, 1996.
- [17] S.M. Carroll, G.B. Field and R. Jackiw, Phys. Rev. D 41 (1990) 1231.
- [18] V.A. Kostelecky and M. Mewes, Phys. Rev. Lett. 87 (2001) 251304.
- [19] R. Jackiw and V.A. Kostelecky, Phys. Rev. Lett. 82 (1999) 3572.
- [20] M. Amoretti et al., Nature 419 (2002) 456.
- [21] M. Amoretti et al., Phys. Lett. B 578 (2004) 23.
- [22] G. Gabrielse et al., Phys. Rev. Lett. 89 (2002) 213401.
- [23] G. Gabrielse et al., Phys. Rev. Lett. 89 (2002) 233401.
- [24] R. Bluhm, V.A. Kostelecky and N. Russell, Phys. Rev. Lett. 79 (1997) 1432.
- [25] A.O. Barvinsky, Yu.V. Gusev, G.A. Vilkovisky and V.V. Zhytnikov, Print-93-0274 (Manitoba), 1993.
- [26] A.O. Barvinsky, Yu.V. Gusev, G.A. Vilkovisky and V.V. Zhytnikov, J. Math. Phys. 35 (1994) 3525; J. Math. Phys. 35 (1994) 3543; Nucl. Phys. B 439 (1995) 561.
- [27] G.M. Shore, Contemp. Phys. 44 (2003) 503.
- [28] F.A. Jenkins and H.E. White, Fundamentals of Optics, McGraw-Hill, N.Y. 1976.

- [29] D.N. Spergel et al, WMAP Collaboration, *Astrophys. J. Suppl.* 148 (2003) 175.
- [30] S. Covino, G. Ghisellini, D. Lazzati and D. Malesani, Polarization of Gamma-ray burst optical and near-infrared afterglows, *astro-ph/0301608*.
- [31] D. Lazzati et al, Intrinsic and dust-induced polarization in gamma-ray burst afterglows: the case of GRB 021004, *astro-ph/0308540*.
- [32] S. Dado, A. Dar and A. De Rújula, On the polarization of gamma ray bursts and their optical afterglows, *astro-ph/0403015*.
- [33] G. Ghisellini and D. Lazzati, Polarization lightcurves and position angle variation of beamed gamma-ray bursts, *astro-ph/9906471*.
- [34] D. Lazzati, Linear Polarization on Gamma-Ray Bursts: from the prompt to the late afterglow, *astro-ph/0312331*.
- [35] C. Itzykson and J-B. Zuber, *Quantum Field Theory*, McGraw-Hill, N.Y. 1985.
- [36] E. Merzbacher, *Quantum Mechanics*, Wiley, N.Y. 1970.
- [37] M. Charlton, J. Eades, D. Horvath, R.J. Hughes and C. Zimmermann, *Phys. Rep.* 241 (1994) 65.
- [38] M.H. Holzschneider et al, *Nucl. Phys. B (Proc. Suppl.)* 56A (1997) 336.
- [39] B. Cagnac, G. Grynberg and F. Biraben, Spectroscopie d'Absorption Multiphonique Sans Effet Doppler, *Journal de Physique* 34 (1973) 845. (In French)
- [40] R. Bluhm, Probing the Planck scale in low-energy atomic physics, *hep-ph/0111323*.
- [41] N.E. Mavromatos, Theoretical and Phenomenological Aspects of CPT Violation, *hep-ph/0305215*.
- [42] M.H. Holzschneider, M. Charlton and M.M. Nieto, *Phys. Rep.* (in press).
- [43] G.F. Bassani, M. Inguscio and T.W. Hansch, eds., *The Hydrogen Atom, Proceedings, Pisa Symposium*, Springer-Verlag, Berlin, Heidelberg, New York, 1988.
- [44] W. Lichten, Hydrogen Spectroscopy and Fundamental Physics, in ref.[43] 39-48.
- [45] M. Allegrini et al, Doppler-Free Two-Photon Spectroscopy of Hydrogen Rydberg States: Rem easurement of R_1 , in ref.[43] 49-60.
- [46] T.W. Hansch, High Resolution Spectroscopy of Hydrogen, in ref.[43] 93-102.